
ON THE NECESSITY OF OUTPUT DISTRIBUTION REWEIGHTING FOR EFFECTIVE CLASS UNLEARNING

Yian Wang*
UIUC
yian3@illinois.edu

Ali Ebrahimpour-Borojeny*
UIUC
ae20@illinois.edu

Hari Sundaram
UIUC
hs1@illinois.edu

ABSTRACT

In this work, we introduce an output-reweighting unlearning method, RWFT, a lightweight technique that erases an entire class from a trained classifier without full retraining. Forgetting specific classes from trained models is essential for enforcing user deletion rights and mitigating harmful or biased predictions. The full retraining is costly and existing unlearning methods fail to replicate the behavior of the retrained models when predicting samples from the unlearned class. We prove this failure by designing a variant of membership inference attacks, MIA-NN that successfully reveals the unlearned class for any of these methods. We propose a simple redistribution of the probability mass for the prediction on the samples in the forgotten class which is robust to MIA-NN. We also introduce a new metric based on the total variation (TV) distance of the prediction probabilities to quantify residual leakage to prevent future methods from susceptibility to the new attack. Through extensive experiments with state of the art baselines in machine unlearning, we show that our approach matches the results of full retraining in both metrics used for evaluation by prior work and the new metric we propose in this work. Compare to state-of-the-art methods, we gain 2.79% in previously used metrics and 111.45% in our new TV-based metric over the best existing method.

1 Introduction

Machine learning models deployed in real-world applications must increasingly support the ability to forget specific information upon request. Class unlearning is particularly challenging because retraining large models from scratch can be prohibitively expensive and it is difficult to change a trained model to completely forget about a learned class or concept. However, privacy regulations such as the EU’s GDPR [Voigt and Von dem Bussche \[2017\]](#) mandate the “right to be forgotten,” enforcing model owners to delete personal data upon request. For instance, in facial recognition systems, all images of a particular individual may constitute a class that must be erased if the person revokes consent. Early methods for machine unlearning primarily expedite the retraining of models at the potential costs of model’s performance [Bourtoule et al. \[2021\]](#). While these methods can be effective, they suffer from high computational overhead or fail to eliminate the influence of the data targeted for removal.

Some other machine unlearning approaches rely on exact methods that are accompanied by certain guarantees. For example, [Izzo et al. \[2021\]](#) introduce an efficient method for deleting data from linear models by adjusting the model parameters directly. [Thudi et al. \[2022\]](#) study unlearning dynamics through the lens of stochastic gradient descent and propose *verification error* as a principled measure of forgetting success. These methods often require specific properties, such as convexity or weight-constrained training, which limits their practicality in deep models. A more practical line of research focuses on approximate methods, that often lack theoretical guarantees but are fast and practical for real-world models. [Golatkar et al. \[2020\]](#) employ fine-tuning techniques with carefully crafted perturbations. [Jia et al. \[2023\]](#) demonstrate that model sparsity can facilitate more efficient unlearning, using pruning to simplify the parameter space. [Foster et al.](#)

*These authors contributed equally to this work

[2024] propose SALUN, a saliency-based technique that identifies and perturbs the most influential weights associated with the forgotten class. Recently, research has shifted toward *class unlearning*, where the goal is to remove an entire semantic class. Warnecke et al. [2021] develop a framework to unlearn both features and labels using influence functions, enabling class-level forgetting in convex models. There are also several existing approximate unlearning methods (e.g., a person, category, or concept) from a model Poppi et al. [2024], Chen et al. [2023], Kodge et al. [2024], Chang et al. [2024], Chen et al. [2024], Panda et al. [2024], Ebrahimpour-Boroojeny et al. [2025].

The setting of class unlearning is different from unlearning random training samples because the unlearned model has to be depleted of any sign of the unlearned class. Failing to consider this difference, we show that the existing methods are susceptible to our newly designed variant of membership inference attacks (MIAs). This vulnerability has remained unnoticed because previously used evaluations and metrics are mainly designed or inspired by prior work on unlearning random subsets of data. To overcome these challenges, we present a simple yet effective method for class unlearning. When a class is marked for removal, we reassign its predicted probability mass proportionally to the remaining classes, preserving the distributional structure of the retrained models. This reweighting mechanism eliminates the model’s ability to predict the forgotten class without altering its internal representations or requiring retraining. Our approach is model-agnostic, efficient, and easy to implement. It can also be incorporated with any prior unlearning methods, such as fine-tuning.

Our method not only exhibits strong robustness against previously-used metrics and MIAs, it also does not fail the evaluations using our newly proposed nearest-neighbor MIA (MIA-NN). We also introduce a new fine-grained metric that not only evaluates the similarity of the prediction probability for the correct label, but also considers this similarity for the other labels by computing the total variation distance (TV) to assess whether the unlearning models replicate the behavior of a retrained models. Our results shows that the unlearned models using our proposed method mirror the behavior of a retrained model, where forgotten class samples are naturally reassigned to semantically similar classes. As a result, the output distributions of the unlearned model closely resemble those of the retrained model, making it significantly harder for adversaries to distinguish forgotten samples.

To evaluate our approach, we conduct comprehensive experiments on MNIST, CIFAR-10, CIFAR-100, and Tiny-ImageNet, comparing against state-of-the-art unlearning methods. We measure performance in terms of retained accuracy, robustness against MIA Hayes et al. [2024], and our newly proposed metric, unlearning total variation (UTV)-distance, which explicitly quantifies the conditional distribution shift between the unlearned and retrained models. Additionally, we present the results for robustness against MIA-NN, which we specifically designed to reveal residual leakage of existing methods missed by standard evaluations.

Our results show that simple output-space interventions effectively approximate retraining performance while significantly reducing computational cost. Specifically, our method achieves up to 5.02% higher remaining accuracy and 16.56% lower unlearning discrepancy than recent state-of-the-art methods such as SVD Foster et al. [2024] and SalUn Kodge et al. [2024], across all datasets. In addition to strong unlearning performance, we conduct a running-time analysis on CIFAR-100 using ResNet-18 (Figure 2 in appendix A.5), demonstrating that our approach achieves substantial computational savings over state-of-the-art baselines demonstrating practicality and scalability. Thus, our contributions can be summarized as follows:

- **Lightweight class unlearning via output reweighting.** We propose a simple yet effective method that removes the influence of a forgotten class by directly modifying the model’s output distribution—either proportionally across retained classes or to the most probable retained class. Unlike prior methods that require retraining Bourtole et al. [2021], model pruning Jia et al. [2023], or architecture-specific weight updates Foster et al. [2024], our approach is model-agnostic and computationally efficient. We accomplish this by applying a post-hoc probability reassignment that preserves the model’s decision boundaries for retained classes. Our method achieves comparable performance to retraining while reducing computation time by an order of magnitude, making it suitable for deployment in real-world systems that demand rapid unlearning.
- **Novel metrics for unlearning evaluation.** To assess fine-grained residual leakage, we introduce two new evaluation tools: (1) Unlearning Total Variance (UTV), which captures distributional shifts between retrained and unlearned models, and (2) MIA-NN, a nearest-class membership inference attack that detects subtle leakage missed by standard MIA tests. In contrast to prior work, which primarily relies on simple accuracy drop or binary membership prediction, our metrics offer deeper insights into how and where leakage persists. Our metrics reveal vulnerabilities in existing baselines and show our approach is robust under stronger adversarial scrutiny, setting a new benchmark for

effective and privacy-preserving unlearning. It is also noteworthy to mention that MIA-NN does not assume any access to the training data, which is a more restrictive assumptions for adversarial attacks.

2 Related Work

In this section, we review prior work on machine and class unlearning, highlighting key approaches such as retraining, fine-tuning, pruning, and representation manipulation.

2.1 Machine Unlearning

Early work on machine unlearning focused on completely retraining models from scratch on the retained data. While accurate, this approach is often impractical for deep networks [Bourtoule et al. \[2021\]](#). Researchers have thus developed approximate methods without full retraining. One line of work uses influence functions to estimate parameter changes from removing specific data points [Warnecke et al. \[2021\]](#), enabling efficient unlearning on entire features or class labels with theoretical guarantees.

Another direction is to approximate data deletion with minimal cost. [Izzo et al. \[2021\]](#) propose a projection-based update for linear and logistic regression models that achieves data deletion in $O(d)$ time. [Thudi et al. \[2022\]](#) unroll the SGD training trajectory to quantify unlearning. And [Jia et al. \[2023\]](#) propose to prune a model before unlearning, which significantly closes the gap between approximate and exact unlearning.

Another category of techniques scrubs specific knowledge from model weights via targeted fine-tuning. [Golatkar et al. \[2020\]](#) propose to inject noise guided by the fisher information matrix to remove information about the forget set. More recently, [Foster et al. \[2024\]](#) proposed Saliency Unlearning (SalUn), which computes a weight saliency map to identify parameters influential in the forgetting set and adjusts only those weights. And [Foster et al. \[2024\]](#) propose selective synaptic damping, which uses fish information to identify and dampen parameters important to the target data.

2.2 Class Unlearning

Recent works tackle the more challenging problem of removing an entire class’s influence while retaining accuracy on other classes. One strategy is to directly adjust the model’s decision boundaries. [Chen et al. \[2023\]](#) propose to shift decision boundaries via fine-tuning on relabeled or pseudo-class data. [Chang et al. \[2024\]](#) propose a Neuron Attribution method using layer-wise relevance propagation to find and perturb class-specific activation paths. And [Shen et al. \[2024\]](#) construct counterfactual samples to unlearn the class by aligning it with random noise representations.

Other strategies involve teacher-student learning and representation subtraction. [Chundawat et al. \[2023\]](#) train a student model through a competent teacher (full knowledge) and an incompetent one (forgetting class). [Tarun et al. \[2023\]](#) apply a two-step impair-repair fine-tuning method to rapidly forget the class. And [Kodge et al. \[2024\]](#) identify forget and retain spaces via singular value decomposition and subtract shared components to remove class-specific features.

In contrast, our approach offers a simple and efficient alternative: directly reweighting the model’s output distribution to eliminate the target class. This intervention cleanly removes the forgotten class while preserving performance on the remaining data.

3 Motivation

To build a precise understanding of unlearning objectives and challenges, we first formalize the problem in section 3.1. In section 3.2, we analyze how a retrained model behaves on forgotten samples—an aspect largely overlooked in prior work—and use this insight to design a stronger variant of MIA that reveals vulnerabilities in existing unlearning techniques.

3.1 Problem Definition: Class Unlearning

Let $\mathcal{D} = \{(\mathbf{x}_i, y_i)\}_{i=1}^N$ be the full training set and let $y_f \in \mathcal{Y}$ denote the class to forget. The forgetting set is defined as $\mathcal{D}_f = \{(\mathbf{x}_i, y_i) \in \mathcal{D} \mid y_i = y_f\}$, and the retained set is $\mathcal{D}_r = \mathcal{D} \setminus \mathcal{D}_f$. The goal of class unlearning is to

produce a model that behaves as if trained only on \mathcal{D}_r , i.e., with no influence from \mathcal{D}_f , while preserving accuracy and privacy on \mathcal{D}_r .

$$p(y = y_f | \mathbf{x}) \approx 0, \quad \forall \mathbf{x} \in \mathcal{X}_f \quad (1)$$

$$p(y = k | \mathbf{x}) \approx p_\theta(y = k | \mathbf{x}), \quad \forall k \neq y_f, \mathbf{x} \in \mathcal{X} \quad (2)$$

where $p_\theta(y | \mathbf{x})$ is the output distribution of the original model, and θ denotes its parameters.

3.2 Observation and MIA-NN Attack

Retrained Model Behavior. Models retrained on \mathcal{D}_r often assign consistent and skewed predictions to \mathcal{D}_f based on semantic similarity. For example, see fig. 1, a model that has never seen automobile samples tends to misclassify them as truck, which is visually and semantically similar. This behavior is not specific to model architecture but emerges from underlying data-level class similarities.

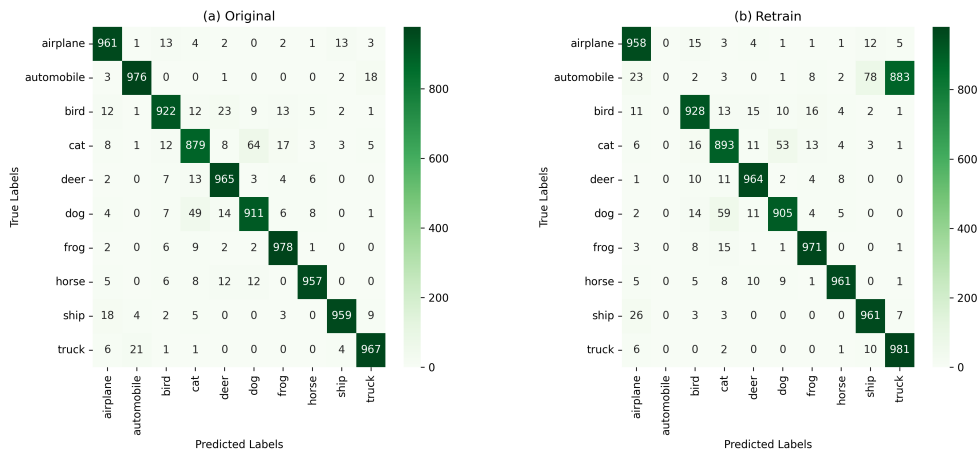


Figure 1: Confusion Matrix for original ResNet18 model and retrained model (forgetting automobile), showing how automobile samples are redirected to similar retained classes (e.g., truck).

Key Insight: Retrained models exhibit structured misclassifications for forgotten classes—typically to semantically close retained classes. Approximate methods that do not replicate this behavior are susceptible to stronger privacy attacks.

MIA-NN: A Targeted Attack. Motivated by this insight, we propose **MIA-NN**, a nearest-neighbor-based membership inference attack that probes whether forgotten class samples are reassigned in a retraining-consistent way.

Setup: We train a binary SVM to distinguish member (truck samples from the test set) vs. non-member (remaining test samples excluding the ones labeled as automobile) samples, using their predicted confidence in belonging to the truck class. We then evaluate the classifier on automobile test samples. If these are not reassigned properly to truck, the SVM detects them as non-members, revealing insufficient unlearning. Ideally, the truck should be identified as members. A more detailed experiment setup is in appendix A.1. From table 1, we observe that our **RWFT-2-O** method achieves the lowest attack success rate among approximate methods, approaching the ideal behavior of retraining and significantly outperforming all other baselines. A detailed introduction of baselines can be seen in section 5.2 and appendix A.2.

Method	retrain	RWFT-2-O	RWFT-O	RW-A	FT	Warnecke et al. [2021]	RL	Golatkar et al. [2020]	GA	Thudi et al. [2022]	SalUn	Foster et al. [2024]	BU	Chen et al. [2023]	Il	Jia et al. [2023]	SVD	Kodge et al. [2024]
Truck MIA Acc	0.0011	0.0310	0.5140	0.0709	0.2209			0.8069		0.7590		0.7680		0.1979		0.9740		0.9440

Table 1: **Membership inference attack accuracy on forgotten class automobile samples via the nearest retained class truck.** Lower values indicate better unlearning (harder to infer membership). **RWFT-2-O** achieves the lowest attack success rate, approaching the ideal behavior of retraining and significantly outperforming all other baselines.

Main Takeaway: Existing methods leak membership under MIA-NN unless they reassign forgotten samples in a retraining-consistent way. Our RWFT variants—especially RWFT-2-O—best match this behavior.

4 Method

In section 4.1, motivated by the observation in section 3.2, we introduce a simple variation of loss that can be used for effective unlearning during the fine-tuning of the model. We will show that by using this loss function, the unlearned model will not be susceptible to the MIA variant. In section 4.2 we elaborate on different strategies that could be used for fine-tuning the model according to our proposed loss function.

4.1 Output Reweighting for Forgetting

Target distribution. Let $p_\theta(y | \mathbf{x})$ be the original model’s output distribution, where θ are the parameters of the pre-trained model. We define the reweighting strategy to remove a target (forget) class y_f :

$$q^*(y | \mathbf{x}) = \begin{cases} 0, & y = y_f, \\ \frac{p_\theta(y | \mathbf{x})}{1 - p_\theta(y_f | \mathbf{x})}, & y \neq y_f. \end{cases} \quad (3)$$

This reweighting preserves the relative proportions of the retained classes by renormalizing the distribution.

Unlearned model. As mentioned earlier, the reweighting strategy can be utilized in any of the prior unlearning methods that utilize iterations of SGD to updated the model Thudi et al. [2022], Warnecke et al. [2021], Jia et al. [2023], Fan et al. [2023]. To show the effectiveness of this strategy, we use it with basic fine-tuning of the model. More specifically, consider probability distribution $p(y | \mathbf{x}) = \text{softmax}(f(\mathbf{x}))$, where $f(\mathbf{x})$ is the feature representation by the model. To unlearn, we fine-tune the model, using any of the strategies in section 4.2, to minimize the following cross-entropy loss on samples from the forget class:

$$\mathcal{L}_{\text{forget}}(\mathbf{x}) = - \sum_{y=1}^K q^*(y | \mathbf{x}) \log p(y | \mathbf{x}). \quad (4)$$

Minimizing this loss drives $p(y_f | \mathbf{x}) \approx 0$, but preserves the distribution over retained classes.

4.2 Training Strategies

The output reweighting framework defined above is general and can be incorporated in most prior work on machine unlearning, including some of the SOTA methods (Fan et al. [2023], Jia et al. [2023]). To show the effectiveness of this strategy, we implement it with simple fine-tuning of the model, without any additional component. We explore three complementary fine-tuning approaches:

1. **Full-Model Fine-Tuning. (RWFT-O)** We directly use the target distribution $q^*(y | \mathbf{x})$ in place of the original soft labels and fine-tune all parameters of the pre-trained network. This end-to-end adaptation encourages global adjustment of decision boundaries while eliminating residual influence of the forget class. Unlike standard fine-tuning Warnecke et al. [2021], which relies on supervision from remaining data \mathcal{D}_r , our method uses an analytically derived target distribution to explicitly reassign the forgotten class’s probability mass without requiring new labels.
2. **Layer-Selective Fine-Tuning. (RWFT-2-O)** Recognizing that different layers capture hierarchical features, we restrict parameter updates to two critical layers: one intermediate convolutional block and the final fully-connected classification layer. By freezing all other layers, this strategy reduces computational cost and mitigates risk of overfitting, while still correcting feature representations relevant to forgetting.
3. **Augmented-Layer Extension. (RWFT-A)** We augment the base architecture with two small trainable layers—one inserted in the middle residual stage and another appended after the final linear layer. This approach preserves the original network parameters intact and concentrates forgetting adjustments in the newly added layers.

All methods minimize the same cross-entropy loss $\mathcal{L}_{\text{forget}}$ defined above, ensuring the forget class probability is driven to zero while preserving the relative probabilities of retained classes.

5 Evaluation Setup

In section 5.1, we elaborate on the datasets and model architectures used in our experiments. In section 5.2 the baseline methods are explained, and in section 5.3 we provide the details on the evaluations metrics used for comparison.

5.1 Datasets and Models

To evaluate the effectiveness of our method, we use three widely used real world image datasets **MNIST** [Deng \[2012\]](#), **CIFAR-10**, and **CIFAR-100** [Krizhevsky et al. \[2009\]](#). Additionally, we extend our evaluation to **TINY-IMAGENET** [Le and Yang \[2015\]](#), a dataset comprising 100,000 images across 200 classes, with each class containing 500 training samples, 50 validation samples, and 50 test samples.

Models For MNIST and CIFAR, we use ResNET18 [He et al. \[2016\]](#) and VGG19 [Simonyan and Zisserman \[2014\]](#) as the original model and for IMAGENET we use the pretrained ResNET18. Full training and hyperparameter configurations are detailed in appendix A.3.

5.2 Baseline Methods

We compare our method against a range of state-of-the-art machine unlearning baselines, including fine-tuning (FT) [Warnecke et al. \[2021\]](#), random labeling (RL) [Golatkar et al. \[2020\]](#), gradient ascent (GA) [Thudi et al. \[2022\]](#), sparse retraining (I1) [Jia et al. \[2023\]](#), boundary unlearning (BU) [Chen et al. \[2023\]](#), saliency-guided unlearning (SalUn) [Fan et al. \[2023\]](#), and SVD-based feature suppression (SVD) [Kodge et al. \[2024\]](#). As a reference, we also include retraining on the retained dataset, commonly considered as the gold standard. Detailed descriptions of all baselines are provided in appendix A.2 and the hyperparameter configurations are detailed in appendix A.3.

5.3 Evaluation Metrics

To assess the effectiveness of our unlearning method, we evaluate the unlearned model using three metrics: the accuracy on the remaining set ACC_r , the accuracy on the forgetting set ACC_f , and the Membership Inference Attack (MIA) score [Shokri et al. \[2017\]](#). We applied the MIA score used by [Kodge et al. \[2024\]](#) due to limited computational resources. Specifically, we leverage the confidence scores of the target class to train a Support Vector Machine (SVM) [Hearst et al. \[1998\]](#) to distinguish between \mathcal{D}_{train_r} (labeled as member class) and \mathcal{D}_{test_r} (labeled as nonmember class). We test this learned model on \mathcal{D}_{train_f} and define the MIA scores as the average model prediction accuracy in classifying the forgetting set \mathcal{D}_{train_f} as nonmembers. A high MIA score indicates the failure of the MIA model to detect \mathcal{D}_{train_f} as a part of training data. Ideally, the MIA score of the unlearned model is expected to match that of the retraining model.

To perform a comprehensive comparison of the effectiveness of the unlearning methods, we utilized a SOTA MIA called RMIA [\[Zarifzadeh et al., 2024\]](#), in addition to using the MIAs from prior works. In RMIA, the area under the ROC curve (AUC) of the MIA scores for predicting the training samples from the unseen samples is reported. Recall that in our setting data is split into four sets: training samples from other classes, training samples from the unlearning class, unseen samples from other classes, and the unseen samples from the unlearning class.

6 Results

In this section, we present a comprehensive empirical evaluation of our proposed unlearning methods across multiple datasets, architectures and various evaluation metrics.

6.1 Main Results

Unlearning Accuracy In table 2, we provide a comprehensive comparison between our approach (ReWeight Fintuning for the whole original model - **RWFT-O**, ReWeight Partial (2-layer) Fintuning for original model

- **RWFT-2-O**, and ReWeight - **RW-A**) and seven existing machine unlearning baselines across two model architectures: VGG19 [Simonyan and Zisserman \[2014\]](#) and ResNet18 [He et al. \[2016\]](#). For single-class forgetting, we report results averaged over different target classes for each dataset. For **MNIST** and **CIFAR-10**, the results are averaged across all 10 classes. For **CIFAR-100**, we compute the average over unlearning experiments conducted on the following 10 classes: *apple, aquarium fish, baby, bear, beaver, bed, bee, beetle, bicycle, and bottle*.

We use *Retrain* as an ideal reference, and assess unlearning methods by how closely they match its performance. In addition to accuracy and privacy metrics, we evaluate the efficiency of our methods in appendix [A.5](#), showing they are significantly faster than full retraining while maintaining comparable unlearning effectiveness. We also perform an ablation study in appendix [A.7](#) to investigate the impact of fine-tuning depth, reassignment strategies and number of forgotten class. Experimental results on the **Tiny-ImageNet-200** dataset are included in appendix [A.4](#) to validate scalability.

Table [2](#) presents the results for single-class forgetting across MNIST, CIFAR-10, CIFAR-100 datasets using VGG19 and ResNet18. Our method consistently achieves perfect forgetting, with $ACC_f = 0$ across all datasets and architectures. Importantly, the retained class accuracy (ACC_r) remains competitive with or superior to baseline unlearning methods, indicating minimal interference with the retained knowledge. Additionally, the MIA scores are either comparable to or better than prior work, suggesting that our method does not compromise membership privacy. These results demonstrate that our approach effectively forgets target classes while preserving utility and privacy for retained data.

MIA Evaluation From Table [2](#), we observe that the original model has near zero MIA score while the retraining model has a score of 100. These are expected as the training forget set \mathcal{D}_{train_f} belongs to the training sample in the original model and is in nonmember class in the retraining model.

We further observe that our method attains the highest MIA score among all unlearning approaches, closely matching that of the retraining baseline, indicating that information related to the forget set has been effectively removed from the model.

6.2 Strong MIA evaluation

We evaluate our method under a strong MIA setting using the U-LIRA framework [Hayes et al. \[2024\]](#), designed to assess whether unlearned models retain residual information about the forgotten class. U-LIRA simulates an adversary with access to shadow models to perform inference attacks on the forget samples.

Following the U-LIRA protocol, we train three shadow models on CIFAR-10 using ResNet18. Each is unlearned with consistent hyperparameters to generate shadow unlearned models. Separately, we retrain three additional models with the forgotten class (e.g., `automobile`) excluded to serve as shadow retrained models. The attacker is trained to distinguish whether a given prediction comes from an unlearned or retrained model based on class-conditional statistics (e.g., mean, variance), and the learned decision boundary is applied in a leave-one-out manner.

We apply the final attack to our actual unlearned model and report the U-LIRA accuracy in table [3](#). A perfect unlearning method should yield 50% accuracy—indicating the attacker cannot distinguish whether forget-class samples came from an unlearned or retrained model. Our RWFT-2-O method is proved to achieve the lowest U-LIRA accuracy among all baselines, demonstrating strong resilience to adaptive attacks and close alignment with ideal unlearning behavior.

6.3 Unlearning Discrepancy

Prior evaluations of class unlearning typically assess forget-class accuracy or MIA confidence scores. However, retrained models on \mathcal{D}_r do not assign labels randomly to forgotten samples—they tend to predict semantically similar classes. For instance, if `automobile` is forgotten in CIFAR-10, retrained models often classify its samples as `truck`. If an unlearned model instead assigns very different labels (e.g., `cat`), it may inadvertently leak information by deviating from retraining behavior. Thus, we propose a stricter evaluation that accounts for distributional alignment with retrained models.

To quantify behavioral differences between the unlearned and retrained models, we define the Unlearning Total Variation (UTV) metric, which computes the average Total Variance distance between their output

Data	Method	VGG19 Simonyan and Zisserman [2014]			ResNet18 He et al. [2016]		
		ACC_r (\uparrow)	ACC_f (\downarrow)	MIA (\uparrow)	ACC_r (\uparrow)	ACC_f (\downarrow)	MIA (\uparrow)
MNIST	Original	99.52 \pm 0.01	99.57 \pm 1.33	0	99.65 \pm 0.04	99.91 \pm 1.05	0.23 \pm 0.23
	Retraining	99.54 \pm 0.03	0	100 \pm 0	99.64 \pm 0.05	0	100 \pm 0
	FT Warnecke et al. [2021]	99.43 \pm 0.72	0	99.25 \pm 0.11	98.16 \pm 0.65	0	95.78 \pm 1.28
	RL Golatkhar et al. [2020]	99.04 \pm 0.19	0	99.66 \pm 0.21	99.33 \pm 0.25	0	99.64 \pm 0.15
	GA Thudi et al. [2022]	97.69 \pm 2.42	0	96.86 \pm 2.87	98.26 \pm 0.12	14.94 \pm 0.03	85.19 \pm 0.17
	l1 Jia et al. [2023]	94.07 \pm 4.48	0.01 \pm 0.02	92.55 \pm 1.53	93.47 \pm 1.98	0.04 \pm 0.02	97.51 \pm 0.42
	BU Chen et al. [2023]	93.14 \pm 8.19	0	95.40 \pm 0.06	94.12 \pm 6.51	0	98.62 \pm 0.15
	SalUn Foster et al. [2024]	99.23 \pm 0.18	0	100 \pm 0	99.43 \pm 0.77	0	100 \pm 0
	SVD Kodge et al. [2024]	99.16 \pm 0.20	0	100 \pm 0	99.37 \pm 0.32	0	99.87 \pm 0.13
	RWFT-O	99.52 \pm 0.07	0	100 \pm 0	99.49 \pm 0.04	0	100 \pm 0
	RWFT-2-O	99.50 \pm 0.02	0	100 \pm 0	99.43 \pm 0.03	0	99.92 \pm 0.11
	RW-A	99.49 \pm 0.02	0	100 \pm 0	99.50 \pm 0.03	0	100 \pm 0
CIFAR-10	Original	92.68 \pm 0.05	92.14 \pm 6.80	0	94.74 \pm 0.09	94.42 \pm 5.45	0.02 \pm 0.02
	Retraining	93.45 \pm 0.10	0	100 \pm 0	94.83 \pm 0.13	0	100 \pm 0
	FT Warnecke et al. [2021]	89.33 \pm 1.86	0	96.94 \pm 0.91	85.60 \pm 2.35	0	96.53 \pm 1.16
	RL Golatkhar et al. [2020]	85.57 \pm 1.29	0	94.07 \pm 0.90	84.74 \pm 4.25	0	94.99 \pm 1.82
	GA Thudi et al. [2022]	87.26 \pm 0.30	14.4 \pm 1.59	97.10 \pm 0.87	90.25 \pm 0.28	14.12 \pm 2.17	96.70 \pm 0.10
	l1 Jia et al. [2023]	90.12 \pm 2.18	0.3 \pm 0.03	92.61 \pm 7.23	93.21 \pm 0.13	0.9 \pm 0.05	100 \pm 0
	BU Chen et al. [2023]	87.32 \pm 3.08	0	85.94 \pm 3.71	87.68 \pm 2.23	0	85.91 \pm 3.97
	SalUn Foster et al. [2024]	89.76 \pm 1.00	0	97.35 \pm 0.65	92.11 \pm 0.65	0	96.33 \pm 2.37
	SVD Kodge et al. [2024]	91.34 \pm 0.45	0	98.10 \pm 1.90	94.17 \pm 0.57	0	97.20 \pm 3.77
	RWFT-O	91.58 \pm 0.23	0	99.26 \pm 0.74	94.28 \pm 0.47	0	97.65 \pm 2.06
	RWFT-2-O	92.30 \pm 0.78	0	99.35 \pm 0.65	94.10 \pm 1.03	0	96.80 \pm 2.80
	RW-A	92.55 \pm 0.10	0	98.16 \pm 1.95	94.61 \pm 1.25	0	97.45 \pm 0.31
CIFAR-100	Original	68.95 \pm 0.72	69.09 \pm 30.27	0.6 \pm 0.6	77.24 \pm 0.14	77.03 \pm 21.24	0.4 \pm 0.4
	Retraining	69.66 \pm 0.87	0	100 \pm 0	77.25 \pm 0.62	0	100 \pm 0
	FT Warnecke et al. [2021]	63.16 \pm 1.17	0	90.08 \pm 2.88	71.37 \pm 1.39	0	91.74 \pm 0.20
	RL Golatkhar et al. [2020]	61.05 \pm 1.17	0	89.54 \pm 2.65	71.31 \pm 1.75	0	89.60 \pm 0.15
	GA Thudi et al. [2022]	56.89 \pm 0.26	0	81.75 \pm 0.37	70.30 \pm 0.05	0	86.25 \pm 0.81
	l1 Jia et al. [2023]	57.02 \pm 0.25	0	81.38 \pm 1.77	70.36 \pm 0.45	0	86.75 \pm 3.32
	BU Chen et al. [2023]	61.34 \pm 4.86	0	86.67 \pm 1.61	68.90 \pm 2.11	0	83.12 \pm 0.59
	SalUn Foster et al. [2024]	62.43 \pm 4.14	0	100 \pm 0	71.02 \pm 1.44	0	100 \pm 0
	SVD Kodge et al. [2024]	67.61 \pm 1.53	0	100 \pm 0	74.31 \pm 1.19	0	98.87 \pm 0.04
	RWFT-O	68.45 \pm 0.41	0	99.10 \pm 0.70	77.13 \pm 0.11	0	99.60 \pm 1.63
	RWFT-2-O	69.25 \pm 0.15	0	100 \pm 0	77.02 \pm 0.42	0	97.80 \pm 2.57
	RW-A	68.90 \pm 0.08	0	99.40 \pm 0.43	76.04 \pm 2.31	0	100 \pm 0

Table 2: **Single-class forgetting on MNIST and CIFAR datasets.** We bold the method with the highest retained accuracy (ACC_r), membership attack robustness (MIA), and lowest forgotten class accuracy (ACC_f). **Our method (RWFT-O, RWFT-2-O, RW-A) consistently achieves perfect forgetting ($ACC_f = 0$), while preserving high retained accuracy and strong MIA robustness across datasets and architectures.** Results are averaged over 10 target classes for each dataset. Retraining results are included as a reference for ideal unlearning behavior.

Metric	RWFT-2-O	RWFT-O	RW-A	FT	RL	GA	SalUn	SVD
U-LIRA Accuracy (%)	68.0	71.12	73.10	72.57	96.79	84.47	97.50	79.30

Table 3: U-LIRA Membership Inference Attack accuracy on CIFAR10 with ResNet18. Lower is better; 50% indicates ideal unlearning. Our finetuning methods RWFT-2-O and RWFT-O achieve the best performance.

distributions on forget-class samples:

$$\text{UTV} = \frac{1}{|\mathcal{D}_f|} \sum_{x \in \mathcal{D}_f} \text{TV}(p_{\theta_r}(y | \mathbf{x}), p_{\theta_u}(y | \mathbf{x})),$$

where θ_r and θ_u are the parameters of the retrained model and unlearned model, respectively.

As shown in table 4, our Reweight Fine-Tuning (RWFT-O) and Reweight (RW-A) approaches deliver the strongest performance.

Metric	RWFT-2-O	RWFT-O	RW-A	FT	RL	GA	SalUn	SVD
UTV	0.0227	0.0252	0.0430	0.0620	0.0898	0.0480	0.0494	0.1883

Table 4: Average Total Variation distance between the unlearned and retrained models on forget-class samples. Lower is better; RWFT-O performs best.

7 Conclusion

We introduce *output-reweighting unlearning*, a lightweight technique that erases an entire class from a pretrained classifier by redistributing the forgotten class’s probability mass while leaving the backbone weights untouched. This preserves decision boundaries for all retained classes and avoids the cost of full retraining.

To quantify how closely an unlearned model is to a fully retrained baseline, we propose *UTV-Unlearning Total Variance distance*, the average total-variation gap between their output distributions on the forget set. We also design a *nearest-class membership-inference attack (MIA-NN)* that utilizes residual mis-mapping of forgotten outputs: previous unlearning methods that pass standard tests fail under this stronger evaluation, whereas our reweighted models remain robust. Experiments on CIFAR-10/100 and Tiny-ImageNet demonstrate that a few epochs of reweight fine-tuning achieve retraining-level performance and is robust to the new attack.

Limitations & Future Work. Our pipeline assumes the forgetting request specifies an exact class label. Extending output-space unlearning to *unknown or mixed-label* forget sets is an open direction. Furthermore, the evidence we provide is entirely empirical. Although the proposed TV-distance metric and nearest-class MIA constitute stronger tests than prior work, they remain heuristic and attack-specific. Deriving provable upper bounds—perhaps by coupling reweighting with certified editing or differential privacy noise [Ginart et al. \[2019\]](#)—under arbitrary, adaptively chosen attacks is an important avenue for future research.

References

- Lucas Bourtole, Varun Chandrasekaran, Christopher A Choquette-Choo, Hengrui Jia, Adelin Travers, Baiwu Zhang, David Lie, and Nicolas Papernot. Machine unlearning. In *2021 IEEE Symposium on Security and Privacy (SP)*, pages 141–159. IEEE, 2021. [1](#), [2](#), [3](#)
- Wenhan Chang, Tianqing Zhu, Yufeng Wu, and Wanlei Zhou. Zero-shot class unlearning via layer-wise relevance analysis and neuronal path perturbation. *arXiv preprint arXiv:2410.23693*, 2024. [2](#), [3](#)
- Huiqiang Chen, Tianqing Zhu, Xin Yu, and Wanlei Zhou. Machine unlearning via null space calibration. *arXiv preprint arXiv:2404.13588*, 2024. [2](#)
- Min Chen, Weizhuo Gao, Gaoyang Liu, Kai Peng, and Chen Wang. Boundary unlearning: Rapid forgetting of deep networks via shifting the decision boundary. In *Proceedings of the IEEE/CVF Conference on Computer Vision and Pattern Recognition*, pages 7766–7775, 2023. [2](#), [3](#), [4](#), [6](#), [8](#)
- Vikram S Chundawat, Ayush K Tarun, Murari Mandal, and Mohan Kankanhalli. Can bad teaching induce forgetting? unlearning in deep networks using an incompetent teacher. In *Proceedings of the AAAI Conference on Artificial Intelligence*, volume 37, pages 7210–7217, 2023. [3](#)
- Li Deng. The mnist database of handwritten digit images for machine learning research [best of the web]. *IEEE signal processing magazine*, 29(6):141–142, 2012. [6](#)

- Ali Ebrahimpour-Borojeny, Hari Sundaram, and Varun Chandrasekaran. Amun: Adversarial machine unlearning. *arXiv preprint arXiv:2503.00917*, 2025. [2](#)
- Chongyu Fan, Jiancheng Liu, Yihua Zhang, Eric Wong, Dennis Wei, and Sijia Liu. Salun: Empowering machine unlearning via gradient-based weight saliency in both image classification and generation. *arXiv preprint arXiv:2310.12508*, 2023. [5](#), [6](#), [2](#)
- Jack Foster, Stefan Schoepf, and Alexandra Brintrup. Fast machine unlearning without retraining through selective synaptic dampening. In *Proceedings of the AAAI conference on artificial intelligence*, volume 38, pages 12043–12051, 2024. [1](#), [2](#), [3](#), [4](#), [8](#)
- Antonio Ginart, Melody Guan, Gregory Valiant, and James Y Zou. Making ai forget you: Data deletion in machine learning. *Advances in neural information processing systems*, 32, 2019. [9](#)
- Aditya Golatkar, Alessandro Achille, and Stefano Soatto. Eternal sunshine of the spotless net: Selective forgetting in deep networks. In *Proceedings of the IEEE/CVF Conference on Computer Vision and Pattern Recognition*, pages 9304–9312, 2020. [1](#), [3](#), [4](#), [6](#), [8](#), [2](#)
- Jamie Hayes, Iliia Shumailov, Eleni Triantafillou, Amr Khalifa, and Nicolas Papernot. Inexact unlearning needs more careful evaluations to avoid a false sense of privacy. *arXiv preprint arXiv:2403.01218*, 2024. [2](#), [7](#)
- Kaiming He, Xiangyu Zhang, Shaoqing Ren, and Jian Sun. Deep residual learning for image recognition. In *Proceedings of the IEEE conference on computer vision and pattern recognition*, pages 770–778, 2016. [6](#), [7](#), [8](#), [2](#)
- Marti A. Hearst, Susan T Dumais, Edgar Osuna, John Platt, and Bernhard Scholkopf. Support vector machines. *IEEE Intelligent Systems and their applications*, 13(4):18–28, 1998. [6](#)
- Zachary Izzo, Mary Anne Smart, Kamalika Chaudhuri, and James Zou. Approximate data deletion from machine learning models. In *International Conference on Artificial Intelligence and Statistics*, pages 2008–2016. PMLR, 2021. [1](#), [3](#)
- Jinghan Jia, Jiancheng Liu, Parikshit Ram, Yuguang Yao, Gaowen Liu, Yang Liu, Pranay Sharma, and Sijia Liu. Model sparsity can simplify machine unlearning. *Advances in Neural Information Processing Systems*, 36: 51584–51605, 2023. [1](#), [2](#), [3](#), [4](#), [5](#), [6](#), [8](#)
- Sangamesh Kodge, Gobinda Saha, and Kaushik Roy. Deep unlearning: Fast and efficient gradient-free class forgetting. *Transactions on Machine Learning Research*, 2024. [2](#), [3](#), [4](#), [6](#), [8](#)
- Alex Krizhevsky, Geoffrey Hinton, et al. Learning multiple layers of features from tiny images. 2009. [6](#)
- Yann Le and Xuan Yang. Tiny imagenet visual recognition challenge. *CS 231N*, 7(7):3, 2015. [6](#)
- Subhodip Panda, Shashwat Sourav, et al. Partially blinded unlearning: Class unlearning for deep networks a bayesian perspective. *arXiv preprint arXiv:2403.16246*, 2024. [2](#)
- Samuele Poppi, Sara Sarto, Marcella Cornia, Lorenzo Baraldi, and Rita Cucchiara. Multi-class unlearning for image classification via weight filtering. *IEEE Intelligent Systems*, 2024. [2](#)
- Shaofei Shen, Chenhao Zhang, Alina Bialkowski, Weitong Chen, and Miao Xu. Camu: Disentangling causal effects in deep model unlearning. In *Proceedings of the 2024 SIAM International Conference on Data Mining (SDM)*, pages 779–787. SIAM, 2024. [3](#)
- Reza Shokri, Marco Stronati, Congzheng Song, and Vitaly Shmatikov. Membership inference attacks against machine learning models. In *2017 IEEE symposium on security and privacy (SP)*, pages 3–18. IEEE, 2017. [6](#)
- Karen Simonyan and Andrew Zisserman. Very deep convolutional networks for large-scale image recognition. *arXiv preprint arXiv:1409.1556*, 2014. [6](#), [7](#), [8](#), [2](#)
- Ayush K Tarun, Vikram S Chundawat, Murari Mandal, and Mohan Kankanhalli. Fast yet effective machine unlearning. *IEEE Transactions on Neural Networks and Learning Systems*, 2023. [3](#)
- Anvith Thudi, Gabriel Deza, Varun Chandrasekaran, and Nicolas Papernot. Unrolling sgd: Understanding factors influencing machine unlearning. In *2022 IEEE 7th European Symposium on Security and Privacy (EuroS&P)*, pages 303–319. IEEE, 2022. [1](#), [3](#), [4](#), [5](#), [6](#), [8](#), [2](#)
- Paul Voigt and Axel Von dem Bussche. The eu general data protection regulation (gdpr). *A Practical Guide, 1st Ed.*, Cham: Springer International Publishing, 10(3152676):10–5555, 2017. [1](#)
- Alexander Warnecke, Lukas Pirch, Christian Wressnegger, and Konrad Rieck. Machine unlearning of features and labels. *arXiv preprint arXiv:2108.11577*, 2021. [2](#), [3](#), [4](#), [5](#), [6](#), [8](#), [1](#)
- Sajjad Zarifzadeh, Philippe Liu, and Reza Shokri. Low-cost high-power membership inference attacks. In *Forty-first International Conference on Machine Learning*, 2024. [6](#)

A Appendix

A.1 Susceptibility to new attacks

A common evaluation technique for approximate unlearning methods—especially those lacking theoretical guarantees—is the membership inference attack (MIA). Traditional MIA approaches typically rely on the model’s confidence in the true class to determine whether a sample was part of the training data. However, as motivated earlier, simply suppressing the output probability of the forgotten class is insufficient. If the remaining output distribution is not properly reweighted, an adversary can still infer the forgotten class via indirect cues—such as a consistent increase in confidence toward a semantically similar retained class (e.g., class `automobile` is predicted as class `truck`).

To capture this vulnerability, we introduce **MIA-NN**, a nearest-neighbor-based attack that exploits residual associations between the forgotten class and its closest retained class. Our method is specifically designed to reveal forgotten samples in unlearned models that would otherwise appear successful under standard MIA evaluations.

Experimental Setup. We evaluate MIA-NN using a ResNet18 model trained on CIFAR-10, where we unlearn the `automobile` class. We select `truck`—a semantically similar retained class—as the nearest neighbor to `automobile` and construct the attack as follows:

- We treat the **truck test samples** as **members** (label 1) since they should yield high confidence in the truck class.
- We treat **non-truck and non-automobile test samples** as **non-members** (label 0).
- We train a binary SVM to distinguish between these two groups using the model’s confidence in the truck class.
- We then evaluate this SVM on the **test automobile samples**. Ideally, if the unlearning method replicates retraining, the model should map forgotten automobile samples to the truck class, making them indistinguishable from true members.

This test highlights whether the unlearning method not only removes the forgotten class but also reassigns its representation appropriately. If the SVM successfully classifies the forgotten automobile samples as members (label 1), it indicates that the model has not sufficiently removed the influence of those samples—despite suppressing their original label. This makes MIA-NN a stronger and more targeted evaluation of class-level unlearning fidelity.

We use a ResNet18 model trained on CIFAR-10 and unlearn the `automobile` class using unlearning methods. We then perform MIA-NN using its nearest retained neighbor, `truck`. Specifically, we:

- Treat the retained training set (excluding trucks) as members (label 1).
- Use the test split of truck images as non-members (label 0).
- Train a binary classifier on these splits, then evaluate it on the forgotten truck samples from the training set.

A.2 Baseline Methods

In this section, we detail several baseline methods for machine unlearning.

Retraining refers to training a new model from scratch using only the retained dataset \mathcal{D}_r . This baseline serves as the ideal unlearning outcome and is commonly regarded as the "gold standard."

Fine-tuning (FT) [Warnecke et al. \[2021\]](#) fine-tunes the source model on the remaining dataset \mathcal{D}_r . In contrast to this standard fine-tuning, our approach performs targeted intervention by adjusting the model’s output distribution to explicitly suppress the forgotten class and reallocate its probability mass proportionally to non-forgotten classes.

Random Labeling (RL) [Golatkhar et al. \[2020\]](#) fine-tunes the model with randomly relabeled forgetting data \mathcal{D}_f , which helps prevent the forgotten data from influencing the model’s predictions.

Gradient Ascent (GA) [Thudi et al. \[2022\]](#) inverts SGD updates to erase the influence of specific training examples.

l1-sparse (l1) Jia et al. [2023] proposes a sparsity-aware unlearning framework that prunes model weights to simplify the parameter space.

Boundary Unlearning (BU) Chen et al. [2023] shifts the decision boundary of the original model to mimic the model’s decisions after retraining from scratch.

SALUN Fan et al. [2023] introduce the concept of weight saliency and perform unlearning by modifying the model weights rather than the entire model, improving effectiveness and efficiency.

SVD Unlearning (SVD) Kodge et al. [2024] performs class unlearning by identifying and suppressing class-discriminative features through singular value decomposition (SVD) of layer-wise activations.

A.3 Experiment Settings

We evaluate our method using two standard architectures: **VGG-19** Simonyan and Zisserman [2014] and **ResNet-18** He et al. [2016]. All models are trained from scratch for **101 - 201 epochs** with a batch size of **128**. Optimization is performed using **stochastic gradient descent (SGD)** with a learning rate of **0.1**, **momentum of 0.9**, and **weight decay of 5×10^{-4}** . The learning rate follows a `torch.optim.lr_scheduler.StepLR` schedule with `step_size = 40` and `gamma = 0.1`.

For our unlearning procedure, we run updates for **10 epochs** with a learning rate of **0.001**. Baseline re-training budgets mirror prior work: GA Thudi et al. [2022], FT Warnecke et al. [2021] and l1 Jia et al. [2023] baselines are run for **20 epochs**, while SalUn is run for **15 epochs**. All experiments are implemented in **PyTorch 2.0** and executed on four **NVIDIA A40 GPUs**, and repeated with three different random seeds; we report the average results across those runs.

A.4 Results on Tiny-ImageNet-200

Method	ResNet-18		
	ACC_r (\uparrow)	ACC_f (\downarrow)	MIA (\uparrow)
Original	63.49	64.52	0
Retrain	63.32	0	100
FT Warnecke et al. [2021]	58.92	0	83.62
RL Golatkar et al. [2020]	41.58	0	83.55
RWFT-A	54.51	0	100
RWFT-O	62.78	0	100
RWFT-2-O	62.84	0	100

Table 5: **Single-class forgetting on Tiny-ImageNet-200 with ResNet-18.** We report retained accuracy (ACC_r), forget accuracy (ACC_f), and membership inference attack accuracy (MIA).

To evaluate unlearning on a more challenging benchmark, we apply our method to the **Tiny-ImageNet-200** dataset using a ResNet-18 backbone. We average the results over 10 semantically diverse classes: *goldfish*, *European fire salamander*, *bullfrog*, *tailed frog*, *American alligator*, *boa constrictor*, *trilobite*, *scorpion*, *black widow spider*, and *tarantula*. Due to computational constraints, we compare against a selected subset of representative baselines. From table 5, we observe that our methods (RWFT-O and RWFT-2-O) achieve perfect forgetting with strong retained accuracy and MIA robustness.

A.5 Running Time Analysis

We compare the wall-clock training time of each unlearning method on the CIFAR-100 dataset using a ResNet-18 backbone, measured on four NVIDIA A40 GPUs. As shown in fig. 2, our proposed **RWFT-2-O** and **RWFT-O** methods are among the fastest, completing in 17.27 and 22.80 minutes respectively—significantly faster than standard retraining-based baselines like FT (s) and RL (30.47 s).

Importantly, all three of our methods — RWFT-2-O, RWFT-O, and RW-A — achieve optimal unlearning performance within just **10 epochs**. This makes them highly efficient and scalable in practice, offering strong privacy guarantees at a fraction of the computational cost of full retraining.

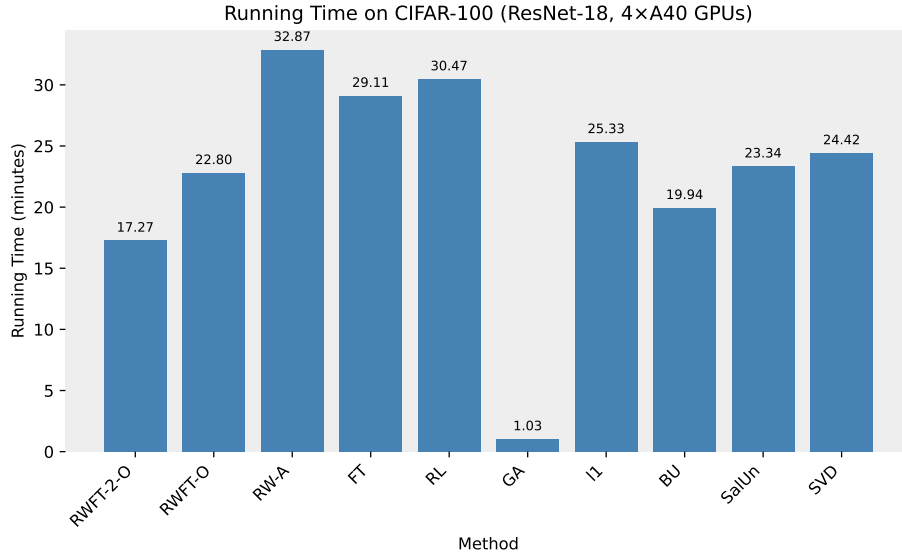


Figure 2: Running time comparison (in seconds) on CIFAR-100 with ResNet-18 using 4x A40 GPUs. Our RWFT-2-O and RWFT-O are among the fastest methods.

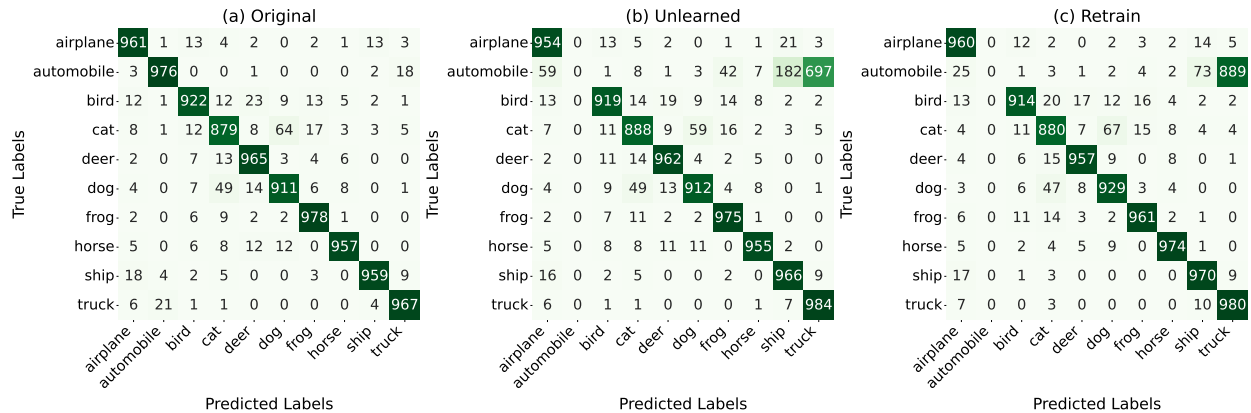


Figure 3: Confusion Matrix for original ResNet18 model, our unlearning model (RWFT-k-O) and retraining model forgetting automobile class, showing redistribution of automobile samples in proportion to the confusion in original model.

A.6 Confusion Matrix analysis

Following [Kodge et al. \[2024\]](#), we plot the confusion matrix showing the distribution of true labels and predicted labels for the original ResNet18 model, our unlearning model (on Automobile) and retraining model for CIFAR10 in [fig. 3](#). Interestingly, we observe that in our unlearning model, a great number of the automobile samples are assigned to 'truck' class, with a small portion being assigned to the 'ship' class, indicating that they share some similar features. This result aligns with that in the retraining model. Furthermore, we see no performance drop in the remaining classes, indicating the robustness of our method.

Forgetting Class Dependency: In addition to evaluating forgetting efficacy through classification accuracy, we further examine where the predictions of forgotten samples are redirected. [Figure 4](#) summarizes the top classes that *willow tree* samples were reassigned to after unlearning. Notably, a significant proportion of the reassigned predictions fall into semantically or visually similar categories, such as *palm tree* (25%), *forest* (17%), and *oak tree* (14%). This suggests that although the model effectively forgets the target class, it redistributes the predictions to classes with similar visual features.

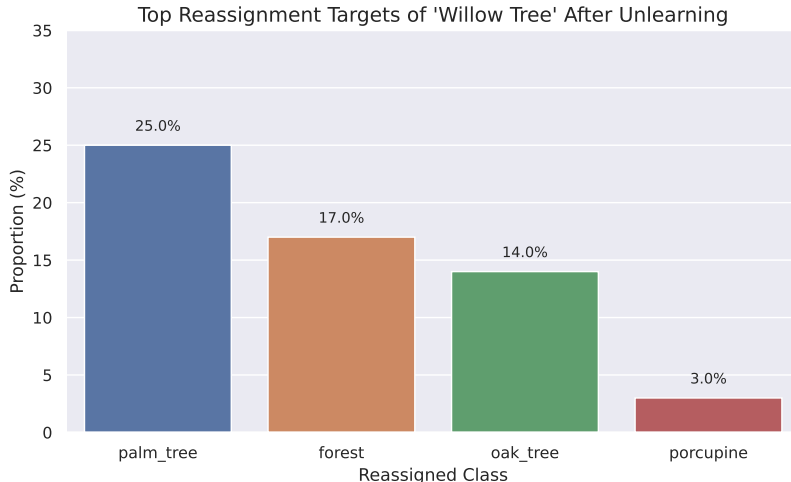


Figure 4: **Top reassignment targets of the forgotten class *willow tree*.** The model tends to reassign samples to semantically similar classes such as *palm tree*, *forest*, and *oak tree*.

Class Name	Original Accuracy (%)	Unlearned Accuracy (%)	Accuracy Drop (%)
maple tree	73.00	47.00	26.00
lion	89.00	82.00	7.00
otter	60.00	53.00	7.00
boy	58.00	52.00	6.00
dinosaur	76.00	71.00	5.00

Table 6: **Top classes with the largest accuracy drop after unlearning the willow tree class in CIFAR100.**

In addition, appendix A.6 highlights the top five classes most affected by the unlearning of the *willow tree* class in CIFAR-100. Notably, *maple tree* suffers the largest performance degradation, with a 26% drop in accuracy. This is followed by moderate drops in *lion*, *otter*, *boy*, and *dinosaur*, which show decreases of 5–7%. These affected classes are likely to share visual similarities with *willow tree*, indicating that the unlearning process may have altered representations that were partially shared across conceptually related categories.

A.7 Ablation Study

Finetuning Across Different Layers

Frozen Layer(s)	$ACC_r \uparrow$	$ACC_f \downarrow$	MIA \uparrow
Layers 1 + Last	91.46 \pm 0.05	0.00	94.85 \pm 0.02
Layers 2 + Last	91.49 \pm 0.07	0.00	95.01 \pm 0.03
Layers 3 + Last	94.10 \pm 1.03	0.00	96.80 \pm 2.80

Table 7: Performance of **RWFT-2-O** with different frozen layers on CIFAR-10 using ResNet-18. Unfreezing deeper layers improves both accuracy and MIA robustness.

To investigate the impact of fine-tuning depth, we conduct an ablation on **RWFT-2-O** by varying which intermediate layers of ResNet-18 are kept trainable during the unlearning phase. As shown in Table 7, unfreezing up to Layer 3 yields the best trade-off, achieving a retained accuracy of 94.10% and the highest MIA resistance at 96.80%. These results suggest that modest adaptation of mid-level feature representations is beneficial for effective unlearning, while freezing earlier layers may hinder alignment with the reweighted output distribution.

Proportional Reassignment vs. Nearest-Class Assignment In section 4.1, we introduced *proportional reassignment*, which redistributes the forgotten class’s probability mass across all retained classes based on their

original proportions. Here, we additionally explore an alternative strategy—*max-class reassignment*—which concentrates the removed mass on the most confident retained class:

$$y_{\max} = \arg \max_{y \neq y_i} p_{\theta}(y | \mathbf{x}), \quad (5)$$

then redistribute the forget mass entirely to y_{\max} :

$$q^*(y | \mathbf{x}) = \begin{cases} 0, & y = y_i, \\ p_{\theta}(y | \mathbf{x}) + p_{\theta}(y_i | \mathbf{x}), & y = y_{\max}, \\ p_{\theta}(y | \mathbf{x}), & \text{otherwise.} \end{cases} \quad (6)$$

This concentrates the removed mass on the single most likely class.

We compare these two reassignment strategies on CIFAR-10 using ResNet18. As shown in Table 8, max-class reassignment tends to yield slightly better retained accuracy, possibly due to better alignment with the model’s natural decision boundaries. However, this comes at a modest cost to membership inference attack (MIA) robustness, as the sharper redistribution may amplify confidence on the reassigned class, making forgotten samples more distinguishable. In contrast, proportional reassignment leads to flatter, more diffused output distributions, which appear harder for an attacker to exploit.

Method	ACC _r ↑	ACC _f ↓	MIA ↑
RW-A (Proportional)	94.61 ± 1.25	0	97.45 ± 0.31
RW-A (Max-class)	94.69 ± 0.08	0	97.30 ± 0.31
RWFT-O (Proportional)	94.28 ± 0.47	0	97.65 ± 2.06
RWFT-O (Max-class)	94.10 ± 0.09	0	96.59 ± 0.39
RWFT-2-O (Proportional)	94.10 ± 1.03	0	96.80 ± 2.80
RWFT-2-O (Max-class)	94.40 ± 0.07	0	96.34 ± 0.11

Table 8: Ablation study on CIFAR-10 using ResNet18: comparing proportional vs. max-class (nearest neighbor) reassignment strategies in reweighting-based unlearning.

Multiple Class Forgetting

Forget Classes	ACC _r ↑	ACC _f ↓	MIA ↑
1 class	77.08 (77.24)	0 (77.03)	100 (0.40)
5 classes	76.95 (77.10)	0 (75.8)	100 (0.96)
10 classes	74.84 (76.66)	0 (77.04)	99.42 (1.23)

Table 9: **Multi-class forgetting performance on CIFAR-100 using ResNet18.** For each setting, we report the accuracy on the retained classes (ACC_r ↑), the accuracy on the forgotten classes (ACC_f ↓), and the MIA attack success rate (MIA ↑). Values in parentheses denote the corresponding metrics from the original (unforgotten) model. **Our method maintains high retained accuracy while fully forgetting target classes and preserving robustness under strong MIAs, demonstrating stable and scalable forgetting performance across varying numbers of classes.**

We evaluated our approach on multi-class forgetting tasks on CIFAR-100 using ResNet18, gradually increasing the number of randomly chosen forgotten classes from 1 to 10. Our method achieves stable and effective forgetting across different numbers of target classes. As shown in Table 9, the retained accuracy (ACC_r) remains consistent with the original model, while the forgotten class accuracy (ACC_f) drops to zero in all cases. Additionally, the MIA attack success rate remains near-perfect, demonstrating that the unlearned model is indistinguishable from retrained baselines even under strong adversarial probing. These results indicate the robustness of our forgetting strategy in multi-class scenarios.